nature communications

Article

https://doi.org/10.1038/s41467-024-53422-y

Local hydroclimate alters interpretation of speleothem $\delta^{18}O$ records

Received: 7 March 2024

Accepted: 8 October 2024

Published online: 21 October 2024

Check for updates

E. W. Patterson[1,10] ✉, V. Skiba[2,3] ✉, A. Wolf[1,11], M. L. Griffiths[4], D. McGee[5], T. N. Bùi[6], M. X. Trần[6], T. H. Đinh[6], Q. Đỗ-Trọng[7], G. R. Goldsmith[8], V. Ersek[9] & K. R. Johnson[1]

Oxygen isotopes ($\delta^{18}O$) are the most commonly utilized speleothem proxy and have provided many foundational records of paleoclimate. Thus, understanding processes affecting speleothem $\delta^{18}O$ is crucial. Yet, prior calcite precipitation (PCP), a process driven by local hydrology, is a widely ignored control of speleothem $\delta^{18}O$. Here we investigate the effects of PCP on a stalagmite $\delta^{18}O$ record from central Vietnam, spanning 45 – 4 ka. We employ a geochemical model that utilizes speleothem Mg/Ca and cave monitoring data to correct the $\delta^{18}O$ record for PCP effects. The resulting record exhibits improved agreement with regional speleothem $\delta^{18}O$ records and climate model simulations, suggesting that the corrected record more accurately reflects precipitation $\delta^{18}O$ ($\delta^{18}O_p$). Without considering PCP, our interpretations of the $\delta^{18}O$ record would have been misleading. To avoid misinterpretations of speleothem $\delta^{18}O$, our results emphasize the necessity of considering PCP as a significant driver of speleothem $\delta^{18}O$.

The effects of karst and in-cave processes on speleothem oxygen isotopes ($\delta^{18}O$) have been largely overlooked when using speleothems for the reconstruction of past climate variability. When precipitated under equilibrium conditions, the primary controls on the $\delta^{18}O$ of speleothem calcite are cave temperature and drip water $\delta^{18}O$, which typically reflects the $\delta^{18}O$ of precipitation ($\delta^{18}O_p$) falling above the cave[1]. Karst hydrology can complicate these signals, but these complexities can often be constrained through hydrological modeling and cave monitoring, and typically only introduce drip water $\delta^{18}O$ variability of < 1 ‰[2,3].

In addition to karst hydrology, in-cave processes affect the fractionation of $\delta^{18}O$ between drip water and calcite[4–8], resulting in the disequilibrium precipitation of most speleothem calcites[9]. Among these processes is prior calcite precipitation (PCP), which refers to all calcite precipitation from infiltrating water prior to speleothem formation. A recent modeling study demonstrated that PCP can theoretically offset speleothem $\delta^{18}O$ by several ‰[4]. This finding raises concerns that PCP could obscure temperature- and $\delta^{18}O_p$-driven speleothem $\delta^{18}O$ variability, making records susceptible to misinterpretation. Given the multitude of published speleothem $\delta^{18}O$ records worldwide[10], there is a critical need to further study this phenomenon.

PCP encompasses all calcite precipitation from infiltrating water prior to the drip water reaching the stalagmite. This includes calcite precipitation in the epikarst, on the cave ceiling, and on an overhanging stalactite or soda straw (Fig. 1)[11,12]. Crucially, PCP changes the geochemical signature of drip water. When CO_2 degasses from drip water, lighter isotopes (^{12}C and ^{16}O) preferentially degas, enriching the

[1]Department of Earth System Science, University of California, Irvine, CA, USA. [2]Potsdam Institute for Climate Impact Research, Member of the Leibniz Association, Potsdam, Germany. [3]Alfred Wegener Institute, Helmholtz Centre for Polar and Marine Research, Potsdam, Germany. [4]Department of Environmental Science, William Paterson University, Wayne, NJ, USA. [5]Department of Earth, Atmospheric and Planetary Sciences, Massachusetts Institute of Technology, Cambridge, MA, USA. [6]Phong Nha- Ke Bang National Park, Phong Nha, Vietnam. [7]University of Science, Vietnam National University, Hanoi, Vietnam. [8]Schmid College of Science and Technology, Chapman University, Orange, California, USA. [9]Department of Geography and Environmental Sciences, Northumbria University, Newcastle, United Kingdom. [10]Present address: Department of Environmental Science, William Paterson University, Wayne, NJ, USA. [11]Present address: Department of Earth and Environmental Sciences, University of Michigan, Ann Arbor, MI, USA. ✉e-mail: pattersone11@wpunj.edu; vanessa.skiba@awi.de

https://doi.org/10.1038/s41467-024-53422-y

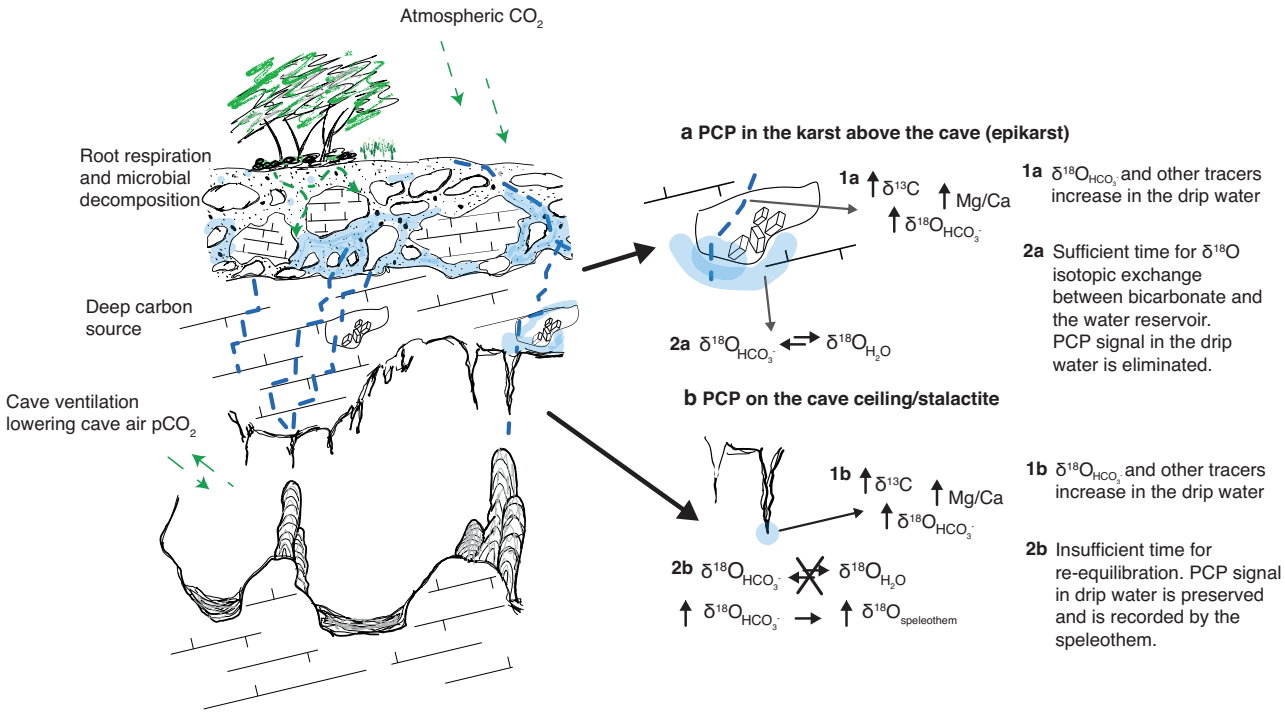

Fig. 1 | Schematic of prior calcite precipitation (PCP) in a cave system. The left panel shows the flow path of drip water and calcite precipitation along the infiltration pathway. Green arrows denote CO_2 fluxes, and blue dashed lines denote water flow. The right panel shows detailed changes in isotopes ($\delta^{18}O$ and $\delta^{13}C$) and trace elements (Mg/Ca) during PCP in (**a**) the epikarst and (**b**) the cave ceiling.

remaining drip water HCO_3^- pool in heavier isotopes (^{13}C and ^{18}O). Cave-analog laboratory experiments show that the calcite that precipitates from the HCO_3^- pool reflects this enriched isotopic signature (higher $\delta^{13}C$ and $\delta^{18}O$ values)[5,13]. Similarly, Mg^{2+} and other trace elements (TEs) with a partition coefficient <1 are preferentially excluded during calcite precipitation[14], with Mg/Ca and other TE/Ca ratios increasing alongside $\delta^{18}O$ and $\delta^{13}C$ in the remaining solution (Fig. 1). Dry conditions enhance PCP because more air in the karst and slower infiltration rates increase the duration of calcite precipitation, leading to stronger enrichment of heavier isotopes and trace element concentrations in the drip water (higher $\delta^{18}O$, $\delta^{13}C$, and Mg/Ca), and hence the speleothem calcite that precipitates from that water. Thus, PCP-sensitive geochemical proxies often reflect local hydroclimate change.

While PCP is a well-known control of speleothem $\delta^{13}C$ and Mg/Ca records[12,14], it is generally not considered when interpreting speleothem $\delta^{18}O$. Traditionally, H_2O exchange - the isotopic re-equilibration between HCO_3^- and the ambient H_2O reservoir - is thought to eliminate the degassing signal (referred to hereafter as the PCP signal) in drip water HCO_3^- $\delta^{18}O$ prior to speleothem formation. With enough time, H_2O exchange, also known as buffering, reestablishes the initial pre-PCP $\delta^{18}O$ value of the drip water HCO_3^- pool, thereby erasing the PCP signature[15]. However, laboratory experiments have demonstrated that H_2O exchange takes much longer than previously estimated[16]. Using the revised estimate of the exchange time, recent modeling studies suggest that speleothem $\delta^{18}O$ does preserve a PCP signal when H_2O isotopic re-equilibration in the drip water is incomplete[4,8]. Importantly, ref. 4 demonstrates that incomplete H_2O exchange is most likely to be preserved by speleothems when PCP occurs on the cave ceiling and/or stalactite. This is because the residence time of drip water in the epikarst far exceeds the time necessary for re-equilibration, whereas the residence time of drip water on the cave ceiling or stalactite may be sufficiently short to maintain isotopic disequilibrium during calcite precipitation.

Although geochemical models successfully simulate the effects of PCP on calcite $\delta^{18}O$, these effects have only recently been observed in speleothem $\delta^{18}O$ records[7,17]. Using a correction method to remove the PCP signal from a speleothem $\delta^{18}O$ record of the Holocene from central Vietnam, ref. 17 found that PCP obscured the $\delta^{18}O_p$ signal in portions of their $\delta^{18}O$ record. They reinterpreted their record using the corrected $\delta^{18}O$, which resolved disagreements in their data and led to a deeper understanding of the local and regional components of the monsoon system in Southeast Asia during the Holocene, a relationship still unresolved over glacial time periods.

Here, we build upon this work by examining the impact of PCP on another previously published $\delta^{18}O$ record from central Vietnam[18]. Using a geochemical model to remove the PCP signal from the speleothem $\delta^{18}O$ record (see *"Methods"*), we demonstrate that PCP overprints the expected $\delta^{18}O_p$ signal in the record. After removing the PCP signal, the corrected $\delta^{18}O$ record shows substantially improved agreement with regional $\delta^{18}O$ speleothem records and climate model output, providing a more accurate estimation of past $\delta^{18}O_p$ variability in central Vietnam from 45 – 4 ka.

Results/discussion

Controls on $\delta^{18}O_p$ in central Vietnam

Central Vietnam receives rainfall from two isotopically distinct monsoon systems, the southwest monsoon (more negative $\delta^{18}O_p$, 30% of annual rainfall from June-August) and the northeast monsoon (more positive $\delta^{18}O_p$, 47% of annual rainfall from September-November) (Fig. 2)[18]. Importantly, large-scale atmospheric processes, rather than local rainfall amounts, control the $\delta^{18}O_p$ of both monsoon systems. Upstream rainout of moisture sourced from the Bay of Bengal and Indian Ocean drives southwest monsoon $\delta^{18}O_p$[19,20]. While northeast monsoon $\delta^{18}O_p$ is not correlated with local rainfall amount[21], the large-scale mechanisms driving its variability are less understood. Annual $\delta^{18}O_p$, the signal recorded by the majority of speleothem records in central Vietnam, reflects a combination of rainfall from these two monsoon systems (seasonality), but not local rainfall amount[21]. On modern timescales, the proportion of southwest vs northeast rainfall amount, which is driven by the timing of the SW-NE wind direction

https://doi.org/10.1038/s41467-024-53422-y

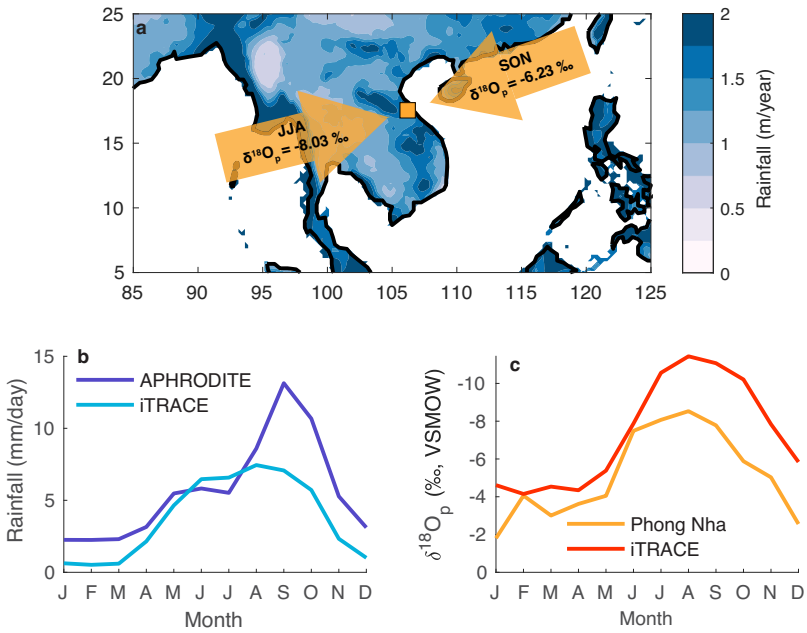

Fig. 2 | Modern and pre-industrial iTRACE climatology. a Map of total annual precipitation in Mainland Southeast Asia derived from Asian Precipitation-Highly Resolved Observational Data Integration Towards Evaluation (APHRODITE)[59]. Arrows show wind direction of the SW monsoon and NE monsoon with average $\delta^{18}O_p$ values of JJA and SON precipitation. The orange square denotes the study site location. The average seasonal cycle of (**b**) rainfall from APHRODITE (dark blue) and iTRACE Pre-industrial simulations (light blue) and (**c**) $\delta^{18}O_p$ measured from rainfall collected at Phong Nha-Ke Bang Park Headquarters (orange) and from iTRACE Pre-industrial simulations (red). APHRODITE and iTRACE time series taken from grid cell encompassing the study site.

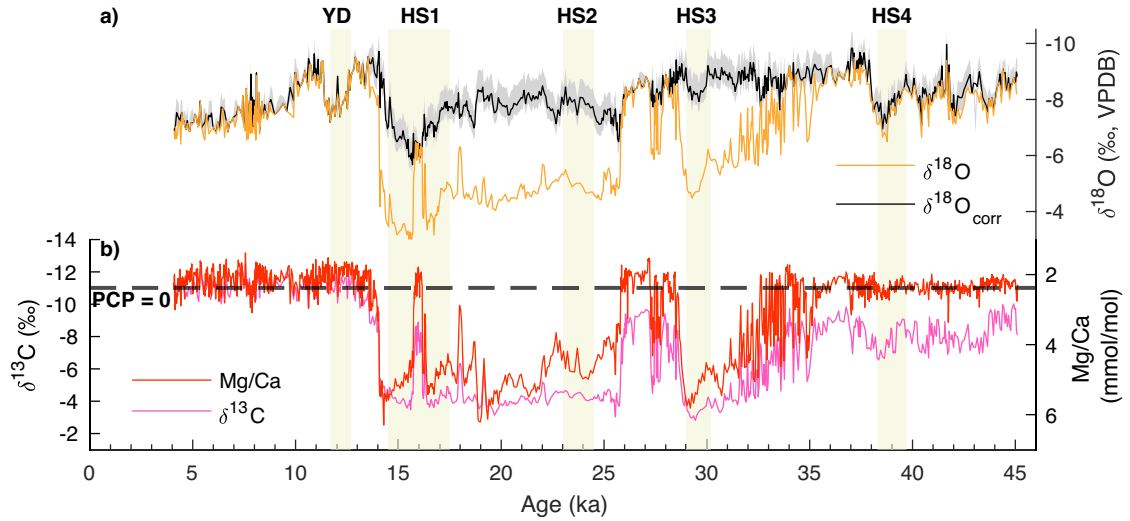

Fig. 3 | Stalagmite (HH-1) proxies from 45 – 4 ka. a HH-1 $\delta^{18}O$ (orange) and corrected $\delta^{18}O$ ($\delta^{18}O_{corr}$, black). The black line is the correction using the best choice parameter configuration (see Supplementary Table S1) and $\alpha_{calcite\text{-}water}$ from ref. 53 (see "*Methods*"). The gray shading denotes the standard deviation of the 1000 Monte Carlo simulations from the sensitivity testing. **b** HH-1 Mg/Ca (red) and $\delta^{13}C$ (pink). The black dashed line shows the Mg/Ca threshold used to determine Mg/Ca_i. Beige shading denotes the Younger Dryas and Heinrich Stadials 1–4. The Mg/Ca, $\delta^{13}C$, and $\delta^{18}O$ curves are from ref. 18.

shift during the southward migration of the ITCZ, controls interannual $\delta^{18}O_p$ variability[21]. However, less is known about central Vietnam $\delta^{18}O_p$ variability on longer timescales.

PCP-corrected $\delta^{18}O$

In this study, we revisit a $\delta^{18}O$ record (~ 50 yr resolution) from a 3.7 m long previously broken stalagmite (HH-1) collected from Hoa Huong cave in Phong Nha-Ke Bang National Park in central Vietnam (Supplementary Figs. S1, S2; 17.5°N, 106.2°E). HH-1 grew continuously from 45 – 4 ka, and the Mg/Ca and $\delta^{13}C$ records were previously used to investigate local hydroclimate change in central Vietnam[18]. A strong correlation between Mg/Ca and $\delta^{13}C$ indicated an important role of local water balance (precipitation minus evapotranspiration) in driving speleothem geochemistry through the PCP mechanism. Notably, the authors also found that HH-1 $\delta^{18}O$ strongly correlated with both $\delta^{13}C$ ($r = 0.79$, $p < 0.01$) and Mg/Ca ($r = 0.87$, $p < 0.01$) records (Fig. 3), suggesting that a common mechanism drove variability in all three proxies. This result was unexpected because $\delta^{18}O_p$ variability in central Vietnam does not reflect local rainfall amount, but rather regional processes such as upstream rainout and seasonality[21]. From this

https://doi.org/10.1038/s41467-024-53422-y

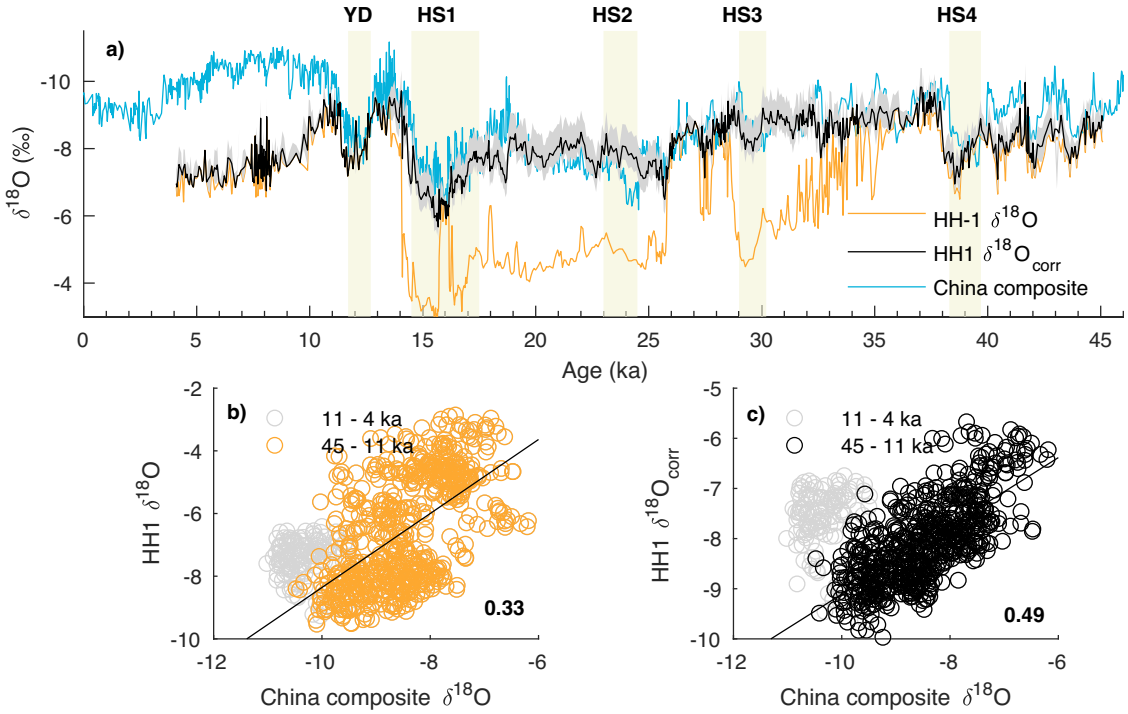

Fig. 4 | HH-1 compared to Chinese stalagmites. a Time series of HH-1 $\delta^{18}O$ (orange), HH-1 $\delta^{18}O_{corr}$ (black), and China composite $\delta^{18}O$ (blue)[22]. Scatter plots of China composite $\delta^{18}O$ vs. **b** HH-1 $\delta^{18}O$ and **c** HH-1 $\delta^{18}O_{corr}$. The Pearson correlation coefficient (r) and Spearman's rank correlation coefficient (ρ) are displayed in the bottom right corner of panels (**b**) and (**c**). For the correlation coefficient values, the China composite record was interpolated to the time steps of the HH-1 record, and Holocene values (gray circles) were excluded. The *p*-values for all coefficients are < 0.01. See Supplementary Table S2 for r values using $\delta^{18}O_{corr}$ derived with different $\alpha_{calcite\text{-}water}$.

observation, the authors hypothesized that PCP, the primary control on the HH-1 $\delta^{13}C$ and Mg/Ca records, likely influenced the HH-1 $\delta^{18}O$ record. We test this hypothesis by using the HH-1 Mg/Ca record, cave monitoring data, and a geochemical model to remove the PCP signal from the HH-1 $\delta^{18}O$ record. The corrected $\delta^{18}O$ record ($\delta^{18}O_{corr}$) should reflect $\delta^{18}O$ changes driven by regional hydroclimate change ($\delta^{18}O_p$) rather than local water balance (PCP), giving a history of central Vietnam $\delta^{18}O_p$ variability from 45 – 4 ka.

Portions of the HH-1 $\delta^{18}O$ and $\delta^{18}O_{corr}$ records are notably different (Fig. 2a and Supplementary Fig. S2), with corrections reaching > 3–4 ‰ in places. Due to uncertainties introduced by choices we make in the correction method, including values of the model parameters, choice of temperature-dependent fractionation factor ($\alpha_{calcite\text{-}water}$), and assumptions about the cave environment (see "*Methods*"), we focus our analyses on large changes (> 1 ‰) in the HH-1 $\delta^{18}O_{corr}$ record. The original $\delta^{18}O$ record ranges from −3 to −10 ‰, whereas the $\delta^{18}O_{corr}$ record has a smaller range of −6 to −10 ‰. Because the correction removes the PCP signal, the largest changes occur during periods of high PCP (high $\delta^{18}O$, $\delta^{13}C$, and Mg/Ca values), while the smallest changes occur during periods of low PCP (low $\delta^{18}O$, $\delta^{13}C$, and Mg/Ca values). Generally, PCP is highest during the sea-level lowstand of the last glacial period and lowest during the sea-level highstands of the Holocene and late MIS 3. Low sea level exposes land adjacent to the study site (Gulf and Tonkin and South China Shelf), which reduces autumn moisture delivery to central Vietnam[18]. Ultimately, this results in smaller corrections during 45 – 35 ka and 13 – 4 ka, and larger corrections during 35 – 30 ka and 25 – 14 ka. The largest exceptions to this sea-level mechanism are two low PCP excursions from 30 – 25 ka and at 16 ka.

Notably, several features that the original $\delta^{18}O$ record shares with the HH-1 Mg/Ca and $\delta^{13}C$ records are no longer apparent. This includes the increasing trend starting at 35 ka and the abrupt shift to lower values at 14 ka. In the Mg/Ca and $\delta^{13}C$ records, both of these features are interpreted to reflect changes in local rainfall amount driven by sea level change[18]. The correction also removes the anomalous negative excursions from 30 – 25 ka and at 16 ka. Features preserved in the $\delta^{18}O_{corr}$ record include positive excursions during the Younger Dryas and Heinrich Stadials 1, 3, and 4. Overall, the $\delta^{18}O_{corr}$ record no longer shows a relationship with sea level change at our site, but the $\delta^{18}O_{corr}$ record remains sensitive to changes in Atlantic Meridional Overturning Circulation (Younger Dryas and Heinrich Stadials). These multi-proxy results now reveal the important differences between local hydrology (Mg/Ca and $\delta^{13}C$) and large-scale hydroclimate ($\delta^{18}O_{corr}$) that were not evident in the original uncorrected data[18].

To test whether HH-1 $\delta^{18}O_{corr}$ tracks the changes in $\delta^{18}O_p$, we compare the HH-1 $\delta^{18}O_{corr}$ record to regional speleothem $\delta^{18}O$ records and isotope-enabled climate model output. Since there are no long speleothem (> 8000 years) $\delta^{18}O$ records from Mainland Southeast Asia, we compared HH-1 $\delta^{18}O_{corr}$ to a composite $\delta^{18}O$ stalagmite record from China, which reflects large-scale Asian summer monsoon strength[22]. Even though these records are somewhat distant from each other, the controls on summer monsoon $\delta^{18}O_p$ are similar (upstream rainout of moisture sourced from the Bay of Bengal and the Indian Ocean)[19–21], which suggests speleothem $\delta^{18}O$ records may covary across the greater region. The China composite shows far better agreement with the HH-1 $\delta^{18}O_{corr}$ record than the original HH-1 $\delta^{18}O$ record (Fig. 4 and Supplementary Table S2). They have similar values and are strongly in phase from 45 – 11 ka. Both show positive excursions during Heinrich Stadials and the Younger Dryas, and negative excursions during some Dansgaard Oeschger Events. Since $\delta^{18}O_p$ is the primary driver of the China composite $\delta^{18}O$ record, its similarities to the HH-1 $\delta^{18}O_{corr}$ indicate that HH-1 $\delta^{18}O_{corr}$ also reflects $\delta^{18}O_p$ variability. Interestingly, these records are antiphased during the early- and mid-Holocene. Since the HH-1 record ends at ~ 4 ka, we are unable to determine whether this antiphasing continues during the late Holocene.

https://doi.org/10.1038/s41467-024-53422-y

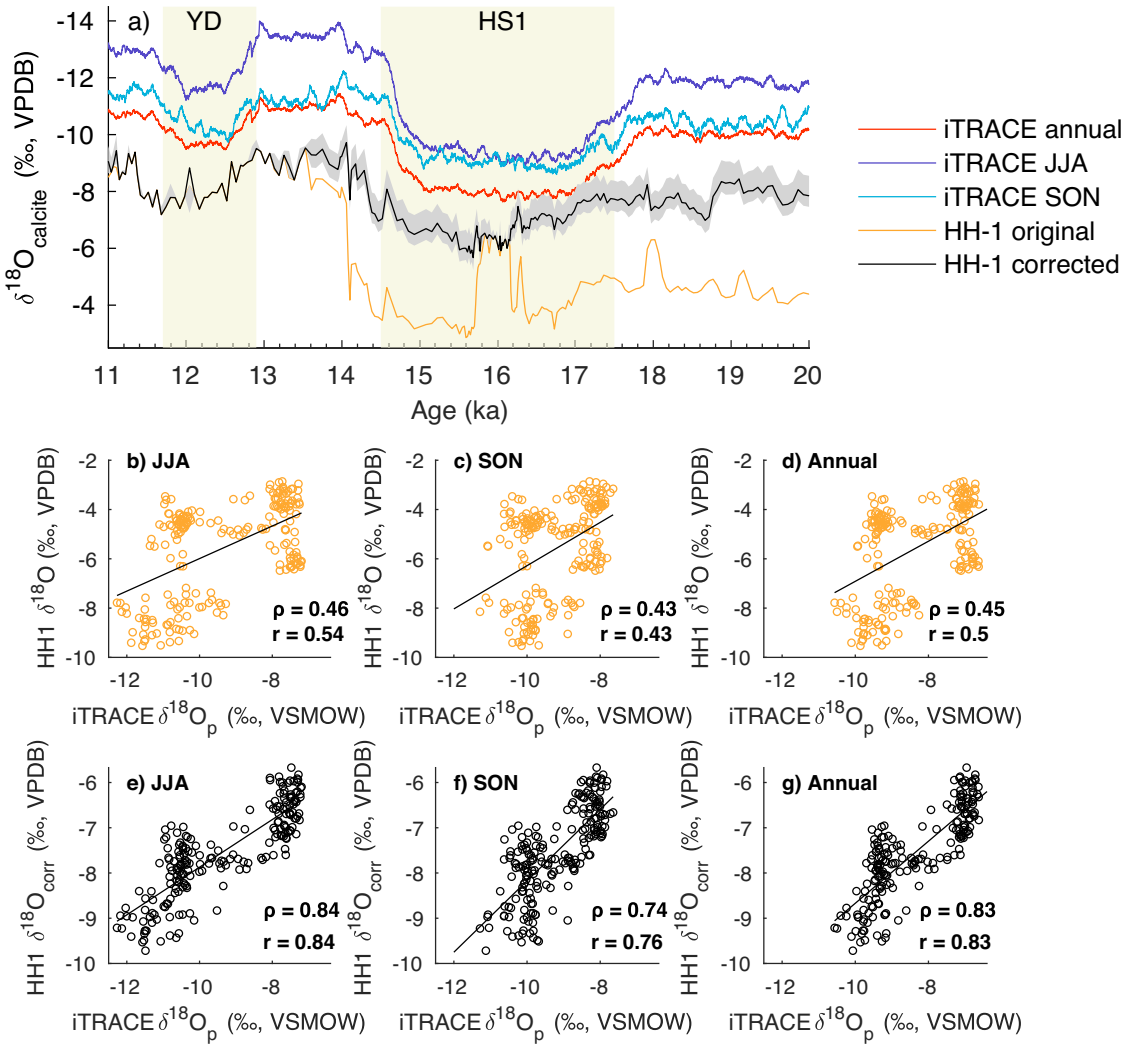

Fig. 5 | HH-1 compared to iTRACE simulations. a Time series of HH-1 $\delta^{18}O$ (orange), HH-1 $\delta^{18}O_{corr}$ (black), iTRACE JJA $\delta^{18}O_c$ (purple), iTRACE SON $\delta^{18}O_c$ (light blue), and iTRACE annual $\delta^{18}O_c$ (red). iTRACE $\delta^{18}O_c$ values (VPDB) calculated from mean weighted iTRACE $\delta^{18}O_p$ (VSMOW) and temperature output using $\alpha_{calcite\text{-}water}$ from ref. 53. For visual clarity, iTRACE curves are smoothed with a 100-year running mean. Scatter plots of iTRACE $\delta^{18}O_p$ vs (**b**–**d**) HH-1 $\delta^{18}O$ (orange) and (**e**–**g**) HH-1 $\delta^{18}O_{corr}$ (black). iTRACE output was smoothed with a 50-year running mean. The Pearson correlation coefficient (r) and Spearman's rank correlation coefficient (ρ) are displayed in the bottom right corner of each panel. The *p*-values for all coefficients are < 0.01. See Supplementary Table S2 for r values using $\delta^{18}O_{corr}$ derived with different $\alpha_{calcite\text{-}water}$.

Given the lack of Late Pleistocene terrestrial $\delta^{18}O$ records from Vietnam, we compare the HH-1 $\delta^{18}O$ record to simulated central Vietnam $\delta^{18}O_p$ from iTRACE[23], an isotope-enabled transient climate model spanning the deglaciation, 20 – 11 ka (see "*Methods*"). Like the comparisons to regional $\delta^{18}O$ records, the JJA (southwest monsoon), SON (northeast monsoon), and annual iTRACE $\delta^{18}O$ time series from the grid cell encompassing the study site better correlate with the HH-1 $\delta^{18}O_{corr}$ record than the original $\delta^{18}O$ record (Fig. 5 and Supplementary Table S2). When converted to $\delta^{18}O$ of calcite ($\delta^{18}O_c$), the simulated iTRACE $\delta^{18}O_c$ time series are more negative than the HH-1 $\delta^{18}O_{corr}$ time series (Fig. 5a). This difference is likely driven by the offset between iTRACE $\delta^{18}O_p$ and $\delta^{18}O_p$ measured from rainfall collected ~15 km from the study site (see "*Methods*"), where iTRACE $\delta^{18}O_p$ is ~1–2 ‰ more negative than observed from July-January (Fig. 2c). Notably, $\delta^{18}O_{corr}$ computed with a cave-derived $\alpha_{calcite\text{-}water}$ (see "*Methods*"), shows a smaller offset (Supplementary Fig. S3), suggesting the choice of $\alpha_{calcite\text{-}water}$ may be important when determining the absolute value of the correction. While the correlation with JJA is highest (Fig. 5e and Supplementary Table S2), the HH-1 $\delta^{18}O_{corr}$ time series better matches the $\delta^{18}O$ magnitude of change in the annual and SON time series (Fig. 5f, g). Nevertheless, the strong agreement between these records suggests that iTRACE correctly simulates $\delta^{18}O_p$ variability in central Vietnam and provides further evidence that the HH-1 $\delta^{18}O_{corr}$ record reflects changes in $\delta^{18}O_p$.

Central Vietnam $\delta^{18}O_p$ variability over the last 45,000 years

We interpret HH-1 $\delta^{18}O_{corr}$ as a record of weighted annual mean $\delta^{18}O_p$ in central Vietnam. Understanding this record is challenging because both southwest monsoon (JJA) and northeast monsoon (SON) rainfall, specifically the relative contribution of each monsoon system, drive modern annual $\delta^{18}O_p$ variability in central Vietnam[21]. This means that HH-1 $\delta^{18}O_{corr}$ variability could reflect changes in JJA $\delta^{18}O_p$, SON $\delta^{18}O_p$, simultaneous changes in both seasons' $\delta^{18}O_p$, and/or changes in precipitation seasonality (e.g., the relative proportion of moisture delivered in autumn vs summer). For this reason, we consider both the southwest and northeast monsoons when interpreting the HH-1 $\delta^{18}O_{corr}$ record.

We first examine $\delta^{18}O_p$ variability during the deglaciation using iTRACE simulations. The similarity between the simulated JJA and SON $\delta^{18}O_p$ time series and their strong correlation with the HH-1 $\delta^{18}O_{corr}$

record makes disentangling the JJA and SON signals difficult (Fig. 5). A previous analysis of iTRACE simulations found that changes in seasonality (the amount of summer vs. autumn rainfall) minimally contributes to annual $\delta^{18}O_p$ change across South China and Southeast Asia[24]. Instead, they show that changes in the isotopic composition of JJA rainfall control annual $\delta^{18}O_p$ variability during the deglaciation, with SON $\delta^{18}O_p$ playing a minor role. However, iTRACE simulations underestimate the SON rainfall amount in central Vietnam (Fig. 2b), suggesting that the model may not capture the full influence of SON rainfall on the annual $\delta^{18}O_p$ signal. Ultimately, the HH-1 $\delta^{18}O_{corr}$ record most closely approximates the values of the annual $\delta^{18}O_p$ simulation (Fig. 5, Supplementary Fig. S3 and Supplementary Table S2), suggesting that our stalagmite likely records the combined $\delta^{18}O_p$ signal of both monsoon seasons.

When we consider the forcings individually, iTRACE $\delta^{18}O_p$ simulations reveal that meltwater forcing drives the majority of $\delta^{18}O_p$ variability during the deglaciation (MWF curve in Supplementary Fig. S4). This includes positive excursions during the HS1 and YD meltwater events, features also present in HH-1. In addition to HS1 and the YD, the HH-1 $\delta^{18}O_{corr}$ record shows positive excursions during Heinrich Stadials 3 and 4, indicating central Vietnam $\delta^{18}O_p$ responds somewhat consistently to meltwater events. The absence of HS2 in the HH-1 record suggests that HS2 is potentially weaker compared to other instances, which aligns with observations made in other paleoclimate records[25,26]. The signature of meltwater events on the Asian summer monsoon is well documented in speleothem $\delta^{18}O$ records[22,27]. During meltwater events, the southward shift of the ITCZ and westerly jet weakens moisture transport[28], which reduces upstream rainout and increases $\delta^{18}O_p$ values across the region[19]. Conversely, the meltwater-driven mechanism on $\delta^{18}O_p$ during SON is currently unknown.

Deciphering the drivers of Holocene $\delta^{18}O_p$ variability from the HH-1 $\delta^{18}O_{corr}$ record is challenging. During the Holocene, speleothem $\delta^{18}O$ records of Asian summer monsoon intensity reach their minimum $\delta^{18}O$ values in the early Holocene (Fig. 4), lagging Northern Hemisphere Summer Insolation by ~ 3 kyrs[22,29]. A recent synthesis of Holocene (8 – 0 ka) Southeast Asian speleothem $\delta^{18}O$ records found the same relationship between the Southeast Asian summer monsoon (southwest monsoon) and summer insolation (PC1 from ref. 17). As for the Southeast Asian northeast monsoon (PC2 from ref. 17), the same study shows that speleothem $\delta^{18}O$ (including a record from central Vietnam) tracks autumn insolation, which peaks in the mid-Holocene. Interestingly, the HH-1 $\delta^{18}O_{corr}$ record resembles neither the southwest nor northeast monsoon but rather has an increasing trend from 11 – 7 ka and then becomes relatively stable from 7 – 4 ka (Supplementary Fig. S5). Notably, the PCP correction is minimal during the Holocene (Fig. 3a), so the uncertainty introduced from the correction method does not explain these differences. It is possible that the correction method underestimates PCP during the Holocene, which would cause $\delta^{18}O_{corr}$ to be too high. While we cannot rule this out, the comparatively low and stable values of the Mg/Ca record indicate that PCP was low during the Holocene, making a large PCP-driven shift in speleothem $\delta^{18}O$ unlikely. In fact, a recent modeling study found that rate-dependent fractionation when the PCP duration is small may decrease calcite $\delta^{18}O$ by up to 0.5 ‰[30]. If this is indeed the case during the Holocene, then PCP would reduce the difference between HH-1 and regional records rather than increase it. Thus, this effect also cannot explain our observed differences. The $\delta^{18}O_{corr}$ record suggests that insolation does not directly drive changes in the HH-1 record $\delta^{18}O$ during the Holocene. Instead, changes in seasonality (JJA versus SON precipitation amount), and changes in the isotopic composition of SON rainfall could both explain HH-1 $\delta^{18}O$ variability during the Holocene (see *Supplementary Text*).

In summary, during the Late Pleistocene, meltwater-forced changes in $\delta^{18}O_p$ drive central Vietnam $\delta^{18}O_p$ variability. With the HH-1 $\delta^{18}O_{corr}$ record deviating from other regional $\delta^{18}O$ records during the Holocene, our understanding of Holocene $\delta^{18}O_p$ variability in central Vietnam is less clear. Moving forward, more $\delta^{18}O$ records from this region, particularly of the Holocene, and more in-depth investigations into autumn monsoon $\delta^{18}O_p$ dynamics are essential.

Implications

Our study emphasizes the potential effects of PCP on a speleothem $\delta^{18}O$ record, which provides insights into our understanding of hydroclimate variability in central Vietnam $\delta^{18}O_p$ from 45 – 4 ka. Without correcting for the effects of PCP, we would have severely misinterpreted the HH-1 $\delta^{18}O$ record. Furthermore, this would have led us to misdiagnose model-proxy disagreement with iTRACE, despite the model performing well. This has important implications, as speleothem $\delta^{18}O$ records are increasingly being used to test paleoclimate model performance[31–33]. While some uncertainties in speleothem $\delta^{18}O$ records are inevitable, it remains essential to address and minimize them to continue improving the utility of speleothem $\delta^{18}O$ records.

Although PCP only affects speleothem $\delta^{18}O$ under certain conditions (when PCP occurs on the cave ceiling or stalactite), future studies should screen for PCP-influenced $\delta^{18}O$ when generating new speleothem records. This could be done through the generation of multiproxy stable isotope and trace elements records from the same speleothem. How widespread the effects of PCP on speleothem $\delta^{18}O$ are is currently unknown; however, PCP is a well-documented driver of many existing $\delta^{13}C$ and trace element records. Generating and interpreting speleothem $\delta^{13}C$ and trace element records and other proxies sensitive to PCP (e.g., Ca isotopes), alongside $\delta^{18}O$ records, could identify whether PCP occurs in drip waters feeding the speleothem sample. As shown in this study, strong similarities between speleothem $\delta^{18}O$ and these proxies are an indicator of PCP-influenced $\delta^{18}O$. Replication with speleothem $\delta^{18}O$ records from the same or nearby caves is another effective screening method since individual drip pathways would not likely be subject to identical PCP histories. If multiple $\delta^{18}O$ records show similar variability, it is unlikely that PCP substantially affects speleothem $\delta^{18}O$.

Furthermore, we show that by utilizing Mg/Ca data and knowledge of the cave environment, it is possible to remove the PCP signal from a speleothem $\delta^{18}O$ record. This method builds upon well-established geochemical relationships and the strong similarity of corrected data with existing records, suggesting it can be reliably used to constrain $\delta^{18}O_p$. However, as detailed in the *Methods*, our model depends on cave monitoring measurements and makes several critical assumptions that may limit its applicability at certain cave sites. While not hugely impactful on the final correction, measurements of cave temperature, epikarst pCO_2, cave pCO_2, drip water $\delta^{18}O$, and the drip interval from an overlying or nearby dripsite are important for constraining the values of the corresponding model parameters. Nevertheless, when cave monitoring data is unavailable or difficult to measure (e.g., epikarst pCO_2), we show that values sourced from the literature and climate model simulations may be suitable substitutes. Although not done in this study, measuring additional proxies, such as fluid inclusion $\delta^{18}O$[34,35], fluid inclusion microthermometry[36], and TEX_{86}[37], would provide estimates of how cave temperature and drip water $\delta^{18}O$ change through time. Of all the parameters in the model, the correction is most sensitive to the initial Mg/Ca value of dripwater (Mg/Ca_i). Since we approximated Mg/Ca_i from a low Mg/Ca threshold in the speleothem Mg/Ca time series, Mg/Ca_i estimated from speleothem records without a clear low-end member may add substantial error to the correction. The choice of $\alpha_{calcite\text{-}water}$ also impacts the correction. In future applications of this method, we recommend performing a sensitivity analysis that includes changing the model parameters and $\alpha_{calcite\text{-}water}$.

The model assumes that PCP is the only driver of speleothem Mg/Ca variability and that all PCP occurs on the cave ceiling. For these reasons, our method may not be suitable for cave sites where there are

multiple controls on speleothem Mg/Ca or where the majority of PCP occurs in the epikarst. Ultimately, further model development and testing in well-monitored caves is needed before widespread application to other PCP-affected speleothem records. Nonetheless, our findings confirm that PCP on cave ceilings can substantially obscure the $\delta^{18}O_p$ signal, potentially leading to the misinterpretation of the widely-used speleothem $\delta^{18}O$ proxy.

Methods

Rainfall $\delta^{18}O$ measurements

A total of 83 rainwater samples were collected from January 2019 - August 2022 at the Phong Nha-Ke Bang National Park headquarters (17.6°N, 106.3°E) using collection methods outlined in ref. 26. We analyzed all samples for $\delta^{18}O$ (VSMOW): 50 at Chapman University (Orange, California) using cavity ring-down spectroscopy (Picarro L2130-i), and 33 at Northumbria University (Newcastle, UK) using off-axis integrated cavity output spectroscopy (Los Gatos Research LWIA-24EP) (Table S3). The long-term standard deviation of an independent quality control standard for each instrument is 0.11 ‰ $\delta^{18}O$ (Picarro) and 0.20 ‰ $\delta^{18}O$ (Los Gatos).

iTRACE

iTRACE is a water isotope-enabled transient simulation of the last deglaciation (20 to 11 ka) performed in iCESM1.3[23,38]. iCESM1.3 is comprised of the Community Atmosphere Model version 1.3 (CAM5.3), the Community Land Model version 4 (CLM4), Parallel Ocean Program version 2 (POP2), and Los Alamos Sea Ice Model version 4 (CICE4). The land and atmosphere resolution is 1.9° x 2.5° (latitude and longitude), with 30 vertical levels in the atmosphere. iTRACE uses four forcing factors: ICE: continental ice sheets that are changed every 1000 years following the ICE-6G model[39] and KMT ocean bathymetry (changed at 14 and 12 ka), ORB: orbital forcing, GHG: greenhouse gas concentrations from ice core reconstructions[40–42], and MWF: meltwater fluxes following TRACE-21ka[43]. These forcings are applied additively to create four parallel simulations (ICE, ICE + ORB, ICE + ORB + GHG, and ICE + ORB + GHG + MWF). The effect of a single forcing can be approximated by subtracting simulations from each other (e.g., ORB = (ICE + ORB) − ICE). Refer to ref. 23 for additional details on the experiment setup and the forcings.

Preindustrial iCESM 1.3 simulations largely capture seasonal changes in rainfall and $\delta^{18}O_p$ in central Vietnam[18]. However, iCESM underestimates autumn rainfall amount by 2–5 mm/day and $\delta^{18}O_p$ by 1–2 ‰ for July-January (Fig. 2b, c). Strong agreement between simulated iTRACE precipitation and the HH-1 Mg/Ca and $\delta^{13}C$ records indicates that iTRACE correctly models centennial-millennial-scale hydroclimate change in central Vietnam across the deglaciation[18].

$\delta^{18}O$ PCP correction

Correction procedure and model description. We corrected the HH-1 $\delta^{18}O$ record for PCP using the HH-1 Mg/Ca time series and following methods from ref. 17. We used a Rayleigh distillation model that simulates $\delta^{18}O$, the evolution of HCO_3^-, and calcite precipitation (represented by the evolution of calcium concentration in the drip water) through time[8,44–46]. This model has three sinks (H_2O, CO_2 degassing, and $CaCO_3$ precipitation), and can account for oxygen isotope exchange between drip water HCO_3^- and the water reservoir (H_2O exchange). The evolution of calcium concentration in the drip water is approximated by exponential decay[47].

Next, we outline the general procedure of the PCP correction method.

1. Estimate PCP duration. We first estimated PCP duration, defined as the length of calcite precipitation (in seconds) in the drip water prior to it reaching the speleothem, for each time point in the Mg/Ca time series with a corresponding $\delta^{18}O$ measurement ($n = 768$, Supplementary Fig. S6a). To do this, we modeled the evolution of calcite precipitation over time, which requires estimates of initial Ca^{2+} concentration (Ca_i) and equilibrium Ca^{2+} concentration (Ca_{eq}) of the drip water, which are determined by the pCO_2 in the soil or karst for Ca_i and the pCO_2 in the cave for Ca_{eq}. For Ca_{eq}, we used measurements of the cave air pCO_2 from Hoa Huong cave (see *Model Parameters section*). For Ca_i, we chose the minimum value necessary to simulate the range of measured Mg/Ca values from HH-1. We started the simulation at an estimated initial Mg/Ca value (Mg/Ca_i, the Mg/Ca of calcite precipitated when the duration of calcite precipitation from the drip water is 0 s, i.e., PCP = 0) and simulated the Mg/Ca evolution over time using a Rayleigh distillation model, with a partition coefficient calculated following ref. 48. We progressively increased Ca_i until the model simulated the Mg/Ca change necessary to explain the maximum Mg/Ca value of the HH-1 record (Supplementary Fig. S7). Thus, the modeled Mg/Ca evolution covers the whole range of Mg/Ca values measured from the HH-1 record and enables us to deduce the PCP duration for each Mg/Ca time point. We give further details on the Mg/Ca_i, Ca_i, and Ca_{eq} values, as well as the partition coefficient, in the *Model Parameters* section. In the Rayleigh model, longer PCP durations lead to increased Mg concentrations in the drip water and the subsequently precipitated calcite, resulting in larger deviations of the corresponding speleothem Mg/Ca from the Mg/Ca_i.

2. Calculate the PCP-induced change in $\delta^{18}O$. We then estimated the PCP-induced change in $\delta^{18}O$ of drip water HCO_3^- for each timepoint using the Mg/Ca-based estimate of PCP duration. To do this, we modeled the oxygen isotope evolution of the HCO_3^- in the drip water and then determined the amplitude of $\delta^{18}O$ change for each sample based on the estimated PCP duration. Similar to the increase in Mg/Ca over the course of calcite precipitation, longer PCP durations will correspond to larger increases in HCO_3^- $\delta^{18}O$ in the Rayleigh model.

3. Calculate $\delta^{18}O_{corr}$. The PCP-induced change in $\delta^{18}O$ for each sample, as calculated in the previous step, was then subtracted from the corresponding measured speleothem $\delta^{18}O$ value to produce the final $\delta^{18}O_{corr}$ time series (Fig. 3a and Supplementary Fig. S2). Ultimately, $\delta^{18}O_{corr}$ should approximate the initial $\delta^{18}O$ value of calcite precipitated in equilibrium with the drip water (when PCP = 0) which is equivalent (in equilibrium with) to the drip water $\delta^{18}O$. In the case of stalagmite HH-1, we expect drip water $\delta^{18}O$ to reflect $\delta^{18}O_p$.

We make two important assumptions in this approach. First, we assume PCP is the only control on drip water Mg/Ca variability. Second, we assume all PCP occurs on the cave ceiling and/or overhanging stalactite. There may be other factors that substantially influence speleothem Mg/Ca (e.g., karst hydrology) and PCP may occur in both the epikarst and on the cave ceiling. We further explore these concepts and how they apply to the correction of the HH-1 $\delta^{18}O$ record in the *Model uncertainty and sensitivity* section.

Model parameters. The model we used for the PCP correction requires a number of parameters as inputs (Mg/Ca_i, cave temperature, Ca_i, Ca_{eq}, drip interval, and drip water $\delta^{18}O$; Supplementary Table S1). When possible, we used direct measurements of the cave environment collected from March 2020 – March 2023 and further described in ref. 18. Otherwise, we used iTRACE model output and values from the literature. To assess the uncertainty of our correction, we also performed sensitivity testing by varying some of the model parameters within realistic ranges. Here, we describe the choices for each parameter.

We used a constant value of 2.23 mmol/mol for Mg/Ca_i (black dashed line in Fig. 3b). We derived this value by averaging two portions of the HH-1 Mg/Ca record (45 – 37 ka, and 13 – 4 ka). For these periods, we assume that little to no PCP occurred based on the comparatively low and relatively stable Mg/Ca values. For sensitivity testing, we varied Mg/Ca_i between 1.96 – 2.5 mmol/mol, based on the standard deviation of the record for the two time periods.

Since the temperature was not constant during the last 45,000 years, we approximated a temperature time series using a combination of cave monitoring data and iTRACE climate model output (Supplementary Fig. S8). We assumed a constant temperature of 21 °C during the Holocene (11 – 4 ka in the HH-1 record), which is an intermediate value between the modern annual temperature of Hoa Huong cave collected via data logger from March 2020 – August 2022 (~ 20 °C[18]) and Holocene (11.1 – 11 ka) iTRACE surface temperature values (~ 21.5 °C). From 20 – 11 ka, we varied temperature based on a 50-year running mean of simulated iTRACE surface temperature from the grid cell encompassing the study site. We used a constant temperature of 18.5 °C for the time period of 45 – 20 ka, based on the annual iTRACE simulated surface temperature from 20 ka. For sensitivity testing, we varied the temperature +/− 2 °C, the current seasonal range in Hoa Huong cave[18].

The model also requires inputs of drip water Ca_i and Ca_{eq}. For our model to explain the full range of HH-1 Mg/Ca values, we had to use a minimum Ca_i value of 3.4 mol/m^3, which is equivalent to a pCO_2 of 49,000 ppm at 21 °C (we assume the same temperature for all the following pCO_2 values). While this value exceeds the majority of soil pCO_2 measurements, pCO_2 levels in the epikarst can surpass those observed at the surface and in the soil. Notably, studies have recorded epikarst pCO_2 values as high as 60,000 – 100,000 ppm[49,50], and studies utilizing geochemical models to approximate epikarst pCO_2 found similarly high levels[51,52] We conducted sensitivity analyses using a range of Ca_i values between 3.4 and 4 mol/m^3 (equivalent to 49,000 – 79,500 ppm) to test how higher epikarst pCO_2 values would affect our results. For Ca_{eq}, we used a value of 0.8 mol/m, which corresponds to a pCO_2 value of 635 ppm, an average of two modern pCO_2 values measured in Hoa Huong Cave, 820 ppm (March 2020) and 510 ppm (March 2023). For the sensitivity testing, we used a range of 0.6–1.4 mmol/m^3, which corresponds to pCO_2 values of 270 – 3400 ppm. Our low estimate of 270 ppm reflects atmospheric conditions during the last glacial maximum[41] and also assumes that the cave is fully ventilated. We based our highest estimate of 3400 ppm on the highest measured value of pCO_2 recorded in August 2022 in Hoa Huong cave.

Drip interval affects speleothem Mg/Ca, and thus, also the PCP duration we estimate with our approach. Since there is no active drip at the collection site, we were unable to measure the drip interval and assume a constant drip interval of 1 drip/second for the method. Even though drip interval may have changed through time, previous work has found changes in drip interval had a smaller effect on the isotopic composition of calcite when compared to the effects of PCP[8].

The model uses an infiltrating water parameter (drip water $\delta^{18}O$) as the initial HCO_3^- $\delta^{18}O$ value. We used iTRACE simulations of weighted annual mean $\delta^{18}O_p$ to estimate the infiltrating water $\delta^{18}O$ parameter (drip water $\delta^{18}O$). We assumed drip water values approximate the weighted annual mean of $\delta^{18}O_p$ because we have limited observations of drip water $\delta^{18}O$ at the study site. From 20 – 11 ka, we varied temperature based on a 50-year running mean of simulated precipitation weighted annual mean $\delta^{18}O_p$ from the grid cell encompassing the study site. We used a constant $\delta^{18}O_p$ value of − 9.4 ‰ for the time period of 45 – 20 ka and − 9.5 ‰ for the time period 11 – 4 ka, based on the iTRACE weighted annual values from 20 ka and 11 ka, respectively. We did not perform sensitivity testing because when PCP duration is sufficiently short (Supplementary Fig. S6a), the effects of the drip water $\delta^{18}O$ value are minimal[8].

We used laboratory-based measurements to calculate the partition coefficient of Mg ($D_{(Mg)}$)[48]. Since $D_{(Mg)}$ is temperature-dependent, we calculated $D_{(Mg)}$ at each time step using the approximated cave temperature record (Fig S8). The model uses temperature-dependent equilibrium fractionation factors (see ref. 8).

Model uncertainty and sensitivity testing. For the sensitivity analyses, we performed 1000 Monte Carlo simulations and determined the standard deviation for each parameter. To assess the uncertainty of the full model, we randomly varied all parameters within the chosen ranges (Supplementary Table S1 and Supplementary Fig. S9a, gray shading on $\delta^{18}O_{corr}$ in Figs. 3–5). To assess the uncertainty of some parameters, we randomly varied a single parameter (Mg/Ca_i, cave temperature, Ca_i, and Ca_{eq}) while keeping the remaining variables constant (Supplementary Fig. S9b–e). For the full model run, the average 1 sigma uncertainty was +/− 0.21 ‰, a relatively small value when compared to the magnitude of variation in the HH-1 $\delta^{18}O_{corr}$ record. Our simulation also revealed that the Mg/Ca_i parameter causes nearly all of the variability in the simulations (Supplementary Fig. S9b). The variability of the remaining variables (temperature, Ca_i, and Ca_{eq}), had negligible effects on the results. This suggests an accurate estimate of Mg/Ca_i is crucial for future use of this correction method.

Given that we do not fully understand how the cave environment changes over time, we assume constant values for several model parameters: Mg/Ca_i, Ca_i, and Ca_{eq}. This assumption is likely incorrect, particularly between glacial and interglacial climate conditions. However, the insensitivity of the PCP correction to changes in Ca_i and Ca_{eq} suggests using constant values for these parameters is reasonable (Supplementary Fig. S9d, e). Conversely, the correction is very sensitive to changes in Mg/Ca_i. Our sensitivity testing accounts for some of this uncertainty, but this is currently a limitation that warrants further investigation. To avoid introducing additional uncertainty to the correction by choosing arbitrary changes in Mg/Ca_i, we use our best estimate of Mg/Ca_i for the entire record.

The sensitivity of the correction to the Mg/Ca_i parameter highlights the importance of the model assumption that PCP is the only driver of drip water Mg/Ca variability. As previously stated, the strong similarities between the HH-1 Mg/Ca and $\delta^{13}C$ records indicate that PCP is the primary control on drip water Mg/Ca[18] (Fig. 3). While we cannot entirely eliminate the influence of other controls on drip water Mg/Ca and whether these controls change through time, the relative stability of the low/no PCP periods in the HH-1 Mg/Ca record during 45 – 37 ka and 13 – 4 ka suggests that factors other than PCP have a negligible effect on Mg/Ca variability.

We test the difference of the PCP corrected $\delta^{18}O$ record when using the fractionation factor ($\alpha_{calcite\text{-}water}$) derived from laboratory experiments[53] against three cave-derived fractionation factors[9,54,55]. The fractionation factor from ref. 53 results in the largest corrections, and the ref. 9 fractionation factor the smallest (Supplementary Fig. S2), and the maximum difference between the resulting $\delta^{18}O_{corr}$ time series is ~ 1 ‰ (Supplementary Fig. S10). Since the different corrections largely do not change the outcome of our interpretations (Supplementary Table S2), we choose to focus our discussion primarily on the PCP correction obtained using the laboratory-derived fractionation factor[53].

We also found that using a version of the model that includes H_2O exchange has a small impact on the correction (Supplementary Fig. S6b). This is because PCP duration for most data points is substantially shorter than the time required for complete H_2O exchange (Supplementary Fig. S6a). For example, only 6 of the 768-time points exceed a PCP duration of 1000 s (orange dashed line in Supplementary Fig. S6a), where H_2O exchange only reduces PCP-induced $\delta^{18}O$ change by ~ 0.35 ‰ (orange dashed line in Supplementary Fig. S6c). In fact, for the majority of the record, the duration of PCP is sufficiently short to render the effects of H_2O exchange negligible.

Importantly, our approach only accounts for PCP occurring immediately prior to speleothem precipitation (i.e., PCP on the cave ceiling or stalactite) and excludes PCP in the epikarst. Since PCP in the epikarst should not affect $\delta^{18}O$[4], we expect the PCP impact on the speleothem $\delta^{18}O$ record to originate from calcite precipitation on the cave ceiling or overlying stalactite. Conversely, PCP in the epikarst *does* affect drip water Mg/Ca as there is no exchange process that counterbalances PCP for Mg/Ca. In cases where PCP occurs in the epikarst,

we would overestimate PCP-induced increase in speleothem $\delta^{18}O$ and bias $\delta^{18}O$ values of the corrected speleothem $\delta^{18}O$ record toward low values. Our correction approach cannot currently disentangle epikarst PCP from in-cave PCP. While there is no stalactite or active drip above HH-1, we do see evidence of a previously connected soda straw on top of HH-1 and some secondary calcite deposits on the cave ceiling, indicating that some form of calcite precipitation likely occurred above the growing stalagmite (Supplementary Fig. S1b). To test the assumption that all PCP occurs on the cave ceiling or in stalactites, we compare our corrected $\delta^{18}O$ record against other regional records less likely to be affected by PCP and climate model output.

Data availability

All corrected $\delta^{18}O$ time series and rainwater $\delta^{18}O$ data from Phong Nha-Ke Bang National Park Headquarters are archived at Zenodo (https://doi.org/10.5281/zenodo.13768949)[56]. The corrected $\delta^{18}O$ time series and the original HH-1 $\delta^{18}O$, $\delta^{13}C$, and Mg/Ca time series can be found at the National Oceanic and Atmospheric Administration National Centers for Environmental Information Paleoclimatology archive (https://doi.org/10.25921/643e-eb71 and https://doi.org/10.5281/zenodo.13768949)[57,58].

Code availability

The code used for the PCP removal method, including instructions and example data, is accessible via Zenodo (https://doi.org/10.5281/zenodo.13768862)[56].

References

1. Lachniet, M. S. Climatic and environmental controls on speleothem oxygen-isotope values. *Quat. Sci. Rev.* **28**, 412–432 (2009).
2. Baker, A. & Bradley, C. Modern stalagmite δ18O: Instrumental calibration and forward modelling. *Glob. Planet. Change* **71**, 201–206 (2010).
3. Treble, P. C. et al. Ubiquitous karst hydrological control on speleothem oxygen isotope variability in a global study. *Commun. Earth Environ.* **3**, 1–10 (2022).
4. Deininger, M. et al. Are oxygen isotope fractionation factors between calcite and water derived from speleothems systematically biased due to prior calcite precipitation (PCP)? *Geochim. Cosmochim. Acta* **305**, 212–227 (2021).
5. Hansen, M., Scholz, D., Schöne, B. R. & Spötl, C. Simulating speleothem growth in the laboratory: Determination of the stable isotope fractionation (δ13C and δ18O) between H2O, DIC and CaCO3. *Chem. Geol.* **509**, 20–44 (2019).
6. Mickler, P. J., Stern, L. A. & Banner, J. L. Large kinetic isotope effects in modern speleothems. *GSA Bull.* **118**, 65–81 (2006).
7. Skiba, V. et al. Millennial-scale climate variability in the Northern Hemisphere influenced glacier dynamics in the Alps around 250,000 years ago. *Commun. Earth Environ.* **4**, 1–10 (2023).
8. Skiba, V. & Fohlmeister, J. Contemporaneously growing speleothems and their value to decipher in-cave processes – A modelling approach. *Geochim. Cosmochim. Acta* **348**, 381–396 (2023).
9. Daëron, M. et al. Most Earth-surface calcites precipitate out of isotopic equilibrium. *Nat. Commun.* **10**, 429 (2019).
10. Kaushal, N. et al. SISALv3: A global speleothem stable isotope and trace element database. *Earth Syst. Sci. Data* **16**, 1933–1963 (2023).
11. Fairchild, I. J. et al. Modification and preservation of environmental signals in speleothems. *Earth Sci. Rev.* **75**, 105–153 (2006).
12. Johnson, K. R., Hu, C., Belshaw, N. S. & Henderson, G. M. Seasonal trace-element and stable-isotope variations in a Chinese speleothem: The potential for high-resolution paleomonsoon reconstruction. *Earth Planet. Sci. Lett.* **244**, 394–407 (2006).
13. Polag, D. et al. Stable isotope fractionation in speleothems: Laboratory experiments. *Chem. Geol.* **279**, 31–39 (2010).
14. Fairchild, I. J. & Treble, P. C. Trace elements in speleothems as recorders of environmental change. *Quat. Sci. Rev.* **28**, 449–468 (2009).
15. Hendy, C. H. The isotopic geochemistry of speleothems—I. The calculation of the effects of different modes of formation on the isotopic composition of speleothems and their applicability as palaeoclimatic indicators. *Geochim. Cosmochim. Acta* **35**, 801–824 (1971).
16. Beck, W. C., Grossman, E. L. & Morse, J. W. Experimental studies of oxygen isotope fractionation in the carbonic acid system at 15°, 25°, and 40 °C. *Geochim. Cosmochim. Acta* **69**, 3493–3503 (2005).
17. Wolf, A. et al. Deciphering local and regional hydroclimate resolves contradicting evidence on the Asian monsoon evolution. *Nat. Commun.* **14**, 5697 (2023).
18. Patterson, E. W. et al. Glacial changes in sea level modulated millennial-scale variability of Southeast Asian autumn monsoon rainfall. *Proc. Natl. Acad. Sci. USA* **120**, e2219489120 (2023).
19. Pausata, F. S. R., Battisti, D. S., Nisancioglu, K. H. & Bitz, C. M. Chinese stalagmite δ18O controlled by changes in the Indian monsoon during a simulated Heinrich event. *Nat. Geosci.* **4**, 474 (2011).
20. Yang, H., Johnson, K. R., Griffiths, M. L. & Yoshimura, K. Interannual controls on oxygen isotope variability in Asian monsoon precipitation and implications for paleoclimate reconstructions. *J. Geophys. Res. D Atmos.* **121**, 8410–8428 (2016).
21. Wolf, A., Roberts, W. H. G., Ersek, V., Johnson, K. R. & Griffiths, M. L. Rainwater isotopes in central Vietnam controlled by two oceanic moisture sources and rainout effects. *Sci. Rep.* **10**, 1–14 (2020).
22. Cheng, H. et al. The Asian monsoon over the past 640,000 years and ice age terminations. *Nature* **534**, 640–646 (2016).
23. He, C. et al. Hydroclimate footprint of pan-Asian monsoon water isotope during the last deglaciation. *Sci. Adv.* **7**, https://doi.org/10.1126/sciadv.abe2611 (2021).
24. He, C. et al. Deglacial variability of South China hydroclimate heavily contributed by autumn rainfall. *Nat. Commun.* **12**, 1–9 (2021).
25. Lynch-Stieglitz, J. et al. Muted change in Atlantic overturning circulation over some glacial-aged Heinrich events. *Nat. Geosci.* **7**, 144–150 (2014).
26. Wright, K. T. et al. Dynamic and thermodynamic influences on precipitation in Northeast Mexico on orbital to millennial timescales. *Nat. Commun.* **14**, 2279 (2023).
27. Zhang, H. et al. East Asian hydroclimate modulated by the position of the westerlies during Termination I. *Science* **362**, 580–583 (2018).
28. Zhang, R. & Delworth, T. L. Simulated tropical response to a substantial weakening of the Atlantic thermohaline circulation. *J. Clim.* **18**, 1853–1860 (2005).
29. Wang, Y. et al. Millennial- and orbital-scale changes in the East Asian monsoon over the past 224,000 years. *Nature* **451**, 1090–1093 (2008).
30. Sade, Z., Hegyi, S., Hansen, M., Scholz, D. & Halevy, I. The effects of drip rate and geometry on the isotopic composition of speleothems: Evaluation with an advection-diffusion-reaction model. *Geochim. Cosmochim. Acta* **317**, 409–432 (2022).
31. Osman, M. B. et al. Globally resolved surface temperatures since the Last Glacial Maximum. *Nature* **599**, 239–244 (2021).
32. Tierney, J. E. et al. Glacial cooling and climate sensitivity revisited. *Nature* **584**, 569–573 (2020).
33. Ramos, R. D. et al. Constraining clouds and convective parameterizations in a climate model using paleoclimate data. *J. Adv. Model. Earth Syst.* **14**, e2021MS002893 (2022).

34. Affolter, S. et al. Central Europe temperature constrained by speleothem fluid inclusion water isotopes over the past 14,000 years. *Sci. Adv.* **5**, https://doi.org/10.1126/sciadv.aav3809 (2019).
35. Fleitmann, D., Burns, S. J., Neff, U., Mangini, A. & Matter, A. Changing moisture sources over the last 330,000 years in Northern Oman from fluid-inclusion evidence in speleothems. *Quat. Res.* **60**, 223–232 (2003).
36. Løland, M. H. et al. Evolution of tropical land temperature across the last glacial termination. *Nat. Commun.* **13**, 5158 (2022).
37. Baker, A. et al. Glycerol dialkyl glycerol tetraethers (GDGT) distributions from soil to cave: Refining the speleothem paleothermometer. *Org. Geochem.* **136**, 103890 (2019).
38. Brady, E. et al. The connected isotopic water cycle in the community earth system model version 1. *J. Adv. Model. Earth Syst.* **11**, 2547–2566 (2019).
39. Peltier, W. R., Argus, D. F. & Drummond, R. Space geodesy constrains ice age terminal deglaciation: The global ICE-6G_C (VM5a) model. *J. Geophys. Res. Solid Earth* **120**, 450–487 (2015).
40. Lüthi, D. et al. High-resolution carbon dioxide concentration record 650,000–800,000 years before present. *Nature* **453**, 379–382 (2008).
41. Petit, J. R. et al. Climate and atmospheric history of the past 420,000 years from the Vostok ice core, Antarctica. *Nature* **399**, 429–436 (1999).
42. Schilt, A. et al. Glacial–interglacial and millennial-scale variations in the atmospheric nitrous oxide concentration during the last 800,000 years. *Quat. Sci. Rev.* **29**, 182–192 (2010).
43. Liu, Z. et al. Transient simulation of last deglaciation with a new mechanism for bølling-allerød warming. *Science* **325**, 310–314 (2009).
44. Deininger, M., Fohlmeister, J., Scholz, D. & Mangini, A. Isotope disequilibrium effects: The influence of evaporation and ventilation effects on the carbon and oxygen isotope composition of speleothems–A model approach. *Geochim. Cosmochim. Acta* **96**, 57–79 (2012).
45. Deininger, M. & Scholz, D. ISOLUTION 1.0: an ISOtope evoLUTION model describing the stable oxygen (δ18O) and carbon (δ13C) isotope values of speleothems. *Int. J. Speleol.* **48**, 21–32 (2019).
46. Scholz, D., Mühlinghaus, C. & Mangini, A. Modelling δ13C and δ18O in the solution layer on stalagmite surfaces. *Geochim. Cosmochim. Acta* **73**, 2592–2602 (2009).
47. Dreybrodt, W. Deposition of calcite from thin films of natural calcareous solutions and the growth of speleothems. *Chem. Geol.* **29**, 89–105 (1980).
48. Day, C. C. & Henderson, G. M. Controls on trace-element partitioning in cave-analogue calcite. *Geochim. Cosmochim. Acta* **120**, 612–627 (2013).
49. Benavente, J. et al. Air carbon dioxide contents in the vadose zone of a Mediterranean Karst. *Vadose Zone J.* **9**, 126 (2010).
50. Peyraube, N., Lastennet, R., Denis, A. & Malaurent, P. Estimation of epikarst air PCO2 using measurements of water δ13CTDIC, cave air PCO2 and δ13CCO2. *Geochim. Cosmochim. Acta* **118**, 1–17 (2013).
51. Baker, A., Flemons, I., Andersen, M. S., Coleborn, K. & Treble, P. C. What determines the calcium concentration of speleothem-forming drip waters? *Glob. Planet. Change* **143**, 152–161 (2016).
52. Treble, P. C. et al. Impacts of cave air ventilation and in-cave prior calcite precipitation on Golgotha Cave dripwater chemistry, southwest Australia. *Quat. Sci. Rev.* **127**, 61–72 (2015).
53. O'Neil, J. R., Clayton, R. N. & Mayeda, T. K. Oxygen isotope fractionation in divalent metal carbonates. *J. Chem. Phys.* **51**, 5547–5558 (1969).
54. Tremaine, D. M., Froelich, P. N. & Wang, Y. Speleothem calcite farmed in situ: Modern calibration of δ18O and δ13C paleoclimate proxies in a continuously-monitored natural cave system. *Geochim. Cosmochim. Acta* **75**, 4929–4950 (2011).
55. Johnston, V., Borsato, A., Spötl, C., Frisia, S. & Miorandi, R. Stable isotopes in caves over altitudinal gradients: fractionation behaviour and inferences for speleothem sensitivity to climate change. *Clim. Past* **9**, 99–118 (2013).
56. Patterson, E. W. et al. Data and code: Local hydroclimate alters interpretation of speleothem δ18O records. Zenodo. https://doi.org/10.5281/zenodo.13768949 (2024).
57. Patterson, E. W. et al. Hoa Huong Cave, Vietnam PCP-Corrected d18O Data from 4-45 ka. National Oceanic and Atmospheric Administration National Centers for Environmental Information Paleoclimatology archive. https://doi.org/10.25921/643e-eb71(2024).
58. Patterson, E. W. et al. Hoa Huong Cave, central Vietnam 4- 45 ka d18O, d13C, and Mg/Ca stalagmite data. National Oceanic and Atmospheric Administration National Centers for Environmental Information Paleoclimatology archive. https://doi.org/10.25921/axna-4s49 (2023).
59. Yatagai, A. et al. APHRODITE: Constructing a long-term daily gridded precipitation dataset for Asia based on a dense network of rain gauges. *Bull. Am. Meteorol. Soc.* **93**, 1401–1415 (2012).

Acknowledgements

We thank the staff and the management board of Phong Nha-Ke Bang National Park, including Mr. D. Nguyen, Mr. H.Q. Nguyen, and Mr. T.V. Vo, for assistance with this project. We also thank D. Limbert and H. Limbert of Oxalis Adventure Tours for providing a map of Hoa Huong Cave and C. He of the University of Miami for providing access to the preindustrial simulations of iTRACE. This work was supported by US NSF P2C2 awards # 2103129/1603056 (K.R.J.), # 2103051/1602947 (M.L.G.), # 2102976 (D.M.), and the Ridge to Reef NSF Research Traineeship award # DGE-1735040 (E.W.P.).

Author contributions

Fieldwork: E.W.P., A.W., K.R.J., M.L.G., T.N.B., M.X.T., T.H.D., Q.D., and V.E. Water isotope analyses: V.E., G.R.G. $\delta^{18}O$ correction model: V.S. Climate model analyses: E.W.P. Visualization: E.W.P., A.W., and V.S. Supervision: K.R.J., M.L.G., and D.M. Writing—original draft: E.W.P., V.S., and A.W. Writing—review & editing: E.W.P., V.S., A.W., M.L.G., D.M., T.N.B., M.X.T., T.H.D., Q.D., G.R.G., V.E., and K.R.J.

Competing interests

The authors declare no competing interests.

Additional information

Supplementary information The online version contains supplementary material available at https://doi.org/10.1038/s41467-024-53422-y.

Correspondence and requests for materials should be addressed to E. W. Patterson or V. Skiba.

Peer review information *Nature Communications* thanks Valdir Novello and the other anonymous reviewers for their contribution to the peer review of this work. A peer review file is available.